Reproductive Biology and Endocrinology

RESEARCH

Open Access

Liraglutide improves follicle development in polycystic ovary syndrome by inhibiting CXCL10 secretion

Min Zhao[1,2,3,4,5†], Baoying Liao[1,2,3,4,5†], Chuyu Yun[1,2,3,4,5], Xinyu Qi[1,2,3,4,5] and Yanli Pang[1,2,3,4,5*]

Abstract

Background At present, a number of clinical trials have been carried out on GLP-1 receptor agonist liraglutide in the treatment of polycystic ovary syndrome (PCOS). However, the effect of liraglutide on follicle development and its specific mechanism are still unclear.

Methods RNA sequencing was used to explore the molecular characteristics of granulosa cells from patients with PCOS treated with liraglutide. The levels of C-X-C motif chemokine ligand 10 (CXCL10) in follicular fluid were detected by ELISA, the expression levels of ovulation related genes and inflammatory factor genes in follicles and granulosa cells were detected by qPCR and the protein levels of connexin 43 (Cx43), Janus Kinase 2 (JAK2) and phosphorylated JAK2 were detected by Western blot. The mouse ovarian follicles culture system in vitro was used to detect the status of follicle development and ovulation.

Results In the present study, we found that liraglutide inhibited the secretion of inflammatory factors in PCOS granulosa cells, among which CXCL10 was the most significant. In addition, CXCL10 was significantly higher in granulosa cells and follicular fluid in PCOS patients than in non-PCOS patients. We applied in vitro follicle culture and other techniques to carry out the mechanism exploration which revealed that CXCL10 disrupted the homeostasis of gap junction protein alpha 1 (GJA1) between oocyte and granulosa cells before physiological ovulation, thus inhibiting follicular development and ovulation. Liraglutide inhibited CXCL10 secretion in PCOS granulosa cells by inhibiting the JAK signaling pathway and can improved dehydroepiandrosterone (DHEA)-induced follicle development disorders, which is reversed by CXCL10 supplementation.

Conclusions The present study suggests that liraglutide inhibits CXCL10 secretion in granulosa cells through JAK signaling pathway, thereby improving the homeostasis of GJA1 between oocyte and granulosa cells before physiological ovulation and ultimately improving the follicular development and ovulation of PCOS, which provides more supportive evidence for the clinical application of liraglutide in the treatment of ovulatory disorders in PCOS.

Trial registration Not applicable.

Keywords Polycystic ovary syndrome, CXCL10, Follicle development, Liraglutide, Gap junction protein alpha 1

†Min Zhao and Baoying Liao contributed equally to this work.

*Correspondence:
Yanli Pang
yanlipang@bjmu.edu.cn

Full list of author information is available at the end of the article

Introduction

Polycystic ovary syndrome (PCOS) is a common reproductive endocrine disease with an incidence rate of 5–10% among women of childbearing age [1]. Women with PCOS are often characterized by hyperandrogenemia, polycystic ovaries and ovulatory disorders. PCOS is the primary cause of anovulatory infertility [2], but its cause is unclear. In addition to impaired fertility, women with PCOS have a greater risk of developing diabetes and cardiovascular diseases than healthy women [3], which impairs the long-term health. At present, PCOS patients are mainly managed with symptomatic treatment, and effective etiological interventions are lacking, indicating the need to explore the pathophysiology of PCOS, which may provide new insights into its treatment.

Follicular development is a complex and precise process that is regulated by various signals, including hormones, paracrine signaling, and bidirectional interactions between oocytes and the surrounding granulosa cells [4]. Intercellular communication between oocytes and granulosa cells plays an important role in follicular development and oocyte maturation. Cumulus cells can maintain contact with oocytes through transzonal projections (TZPs) and provide essential nutrients for their growth and development. In addition, gap junctions between granulosa cells and oocytes are essential for maintaining the meiotic arrest of oocytes [5]. PCOS patients exhibit abnormal follicular development, which mainly manifests as the arrest of small antral follicles and the disrupted formation of dominant follicles, leading to ovulatory dysfunction. Studies have shown that the environmental endocrine disruptor tributyltin (TBT) can inhibit the formation of TZP and block intercellular interactions between granulosa cells and oocytes, thus leading to abnormal follicular growth and the development of PCOS [6]. Additionally, oocyte-granulosa cell gap junction communication and connexin expression were decreased in a type 1 diabetic mouse model [7], indicating a possible correlation between metabolic disorders and oocyte-granulosa cell gap junctions. Therefore, disrupted oocyte–granulosa cell interactions may contribute to ovulatory disorders in PCOS patients, but the specific mechanism involved is unknown, and further exploration is needed.

The ovarian immune microenvironment plays an essential role in follicle development. The number of ovarian resident immune cells has been reported to be limited prior to the luteinizing hormone (LH) surge. During the ovulation process, a rapid influx of immune cells from the circulating blood and the spleen occurs just a few hours after the LH surge [8, 9], indicating that the ovulation process relies on this short-duration and high-intensity local inflammation to some extent. However, persistent chronic inflammation may impair follicle development and ovulation. PCOS in women is characterized by chronic systemic inflammation involving increased serum levels of inflammatory factors, including tumor necrosis factor α (TNF-α), interleukin 18 (IL-18), and interleukin 6 (IL-6) [10]. Therefore, chronic inflammation in local ovaries is a critical contributing factor to ovulatory disorders in PCOS patients, and exploring the impact of local inflammatory factors on follicle development and ovulation could be essential for understanding the pathogenesis of PCOS. As a GLP-1 receptor agonist, liraglutide exerts evident metabolic protective effect and shows promising potential for PCOS treatment. Recent studies indicated that liraglutide may also inhibit the development of chronic inflammation in PCOS, while the local effect of liraglutide on ovaries is still not clear.

In the present study, we compared the transcriptome data of granulosa cells treated with or without liraglutide and found that liraglutide can reduce the expression of various inflammatory factors, among which CXCL10 has the most significant change. CXCL10 is a pro-inflammatory chemokine, which is involved in the occurrence of various metabolic and inflammatory diseases. We measured the levels of the CXCL10 in the follicular fluid of control subjects and PCOS patients and then clarified the impact of increased CXCL10 levels and impaired oocyte-granulosa cell junctions on follicle development via an in vitro follicle culture system. Furthermore, liraglutide was administered to DHEA-treated follicles to validate the therapeutic effect on follicle development and ovulation. RNA-seq also revealed the specific mechanism of the therapeutic effect of liraglutide through decreasing CXCL10 levels, which offers new insights into the inflammation-related mechanism of ovulatory disorder in PCOS and provides additional evidence for the application of liraglutide in PCOS treatment.

Results

Liraglutide inhibited the secretion of CXCL10 in PCOS granulosa cells

As a GLP-1 receptor agonist, liraglutide has been used for the treatment of weight loss and type 2 diabetes, and several clinical trials of liraglutide have been conducted for the treatment of PCOS. Therefore, we further explored the effect of liraglutide on the function of granulosa cells in PCOS patients. First, the RNA-seq results suggested that after liraglutide treatment, the transcription of PCOS granulosa cells significantly changed (Fig. 1A). A volcano plot showed that *CXCL10* was significantly downregulated by liraglutide treatment (Fig. 1B). In addition, the expression of other inflammatory factors including *IL6*, *IL1B* and *CXCL8* was downregulated (Fig. 1C), and the qPCR results in granulosa cells were consistent with the RNA-seq results (Fig. 1D). Finally, we detected the levels of CXCL10 in the granulosa cell

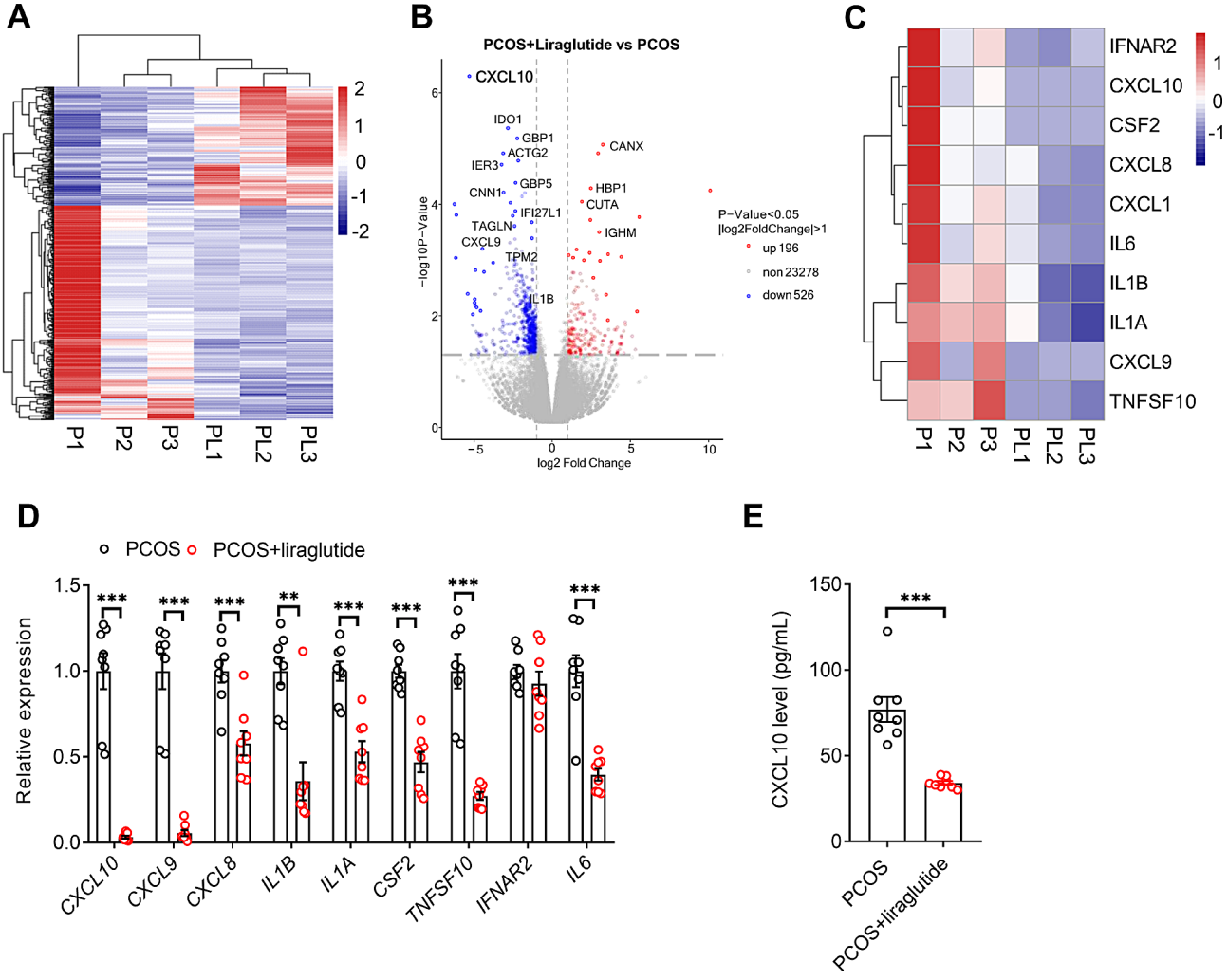

Fig. 1 Liraglutide inhibited the secretion of CXCL10 in PCOS granulosa cells. (**A**) Heatmap of differentially expressed genes (DEGs) in PCOS granulosa cells (P) and PCOS granulosa cells incubated with liraglutide (PL) group. (**B**) Volcano plot showing the significantly DEGs in PCOS + liraglutide group compared to PCOS group, with red spot representing significantly up-regulated genes and blue spot representing significantly down-regulated genes. DEGs were defined as *P* value < 0.05 and log2 fold change > 1. (**C**) Heatmap of DEGs associated with inflammatory factors in the PCOS and PL groups. (**D**) mRNA expression levels of inflammatory factors in human granulosa cells from the PCOS and PL groups; *n* = 8. (**E**) CXCL10 levels in cell culture supernatant after incubated with control and Liraglutide in human granulosa cell of PCOS patients; *n* = 8. For (*CXCL8*, *IL1A*, *CSF2*, *TNFSF10*, *IFNAR2*, *IL6* in **D**), *P* values were determined by two-tailed Student's t- test. For (*CXCL10*, *CXCL9*, *IL1B* in **D**, **E**), *P* values was determined by a two-tailed Mann–Whitney U test. All the data are presented as the mean ± SEM. For D&E, $^{**}P < 0.01$, $^{***}P < 0.001$

Table 1 Clinical characteristics of women with PCOS and controls

	Control (*n* = 20)	PCOS (*n* = 20)	*P* value
Age(year)	32.95 ± 4.11	31.85 ± 3.233	0.353
Body Mass Index	21.43 ± 2.58	23.93 ± 5.18	0.078
FSH(mIU/mL)	6.20 ± 2.73	6.06 ± 1.94	0.853
LH(mIU/mL)	3.64 ± 2.02	6.08 ± 3.46	0.010
LH/FSH	0.60 ± 0.25	1.02 ± 0.55	0.005
Estradiol(pmol/mL)	107.43 ± 39.19	116.15 ± 40.34	0.493
Testosterone(nmol/L)	0.65 ± 0.15	0.93 ± 0.35	0.004
Androstenedione(nmol/L)	5.38 ± 2.13	8.38 ± 2.97	0.004

FSH: Follicle stimulating hormone; LH: Luteinizing hormone. All data are expressed as the mean ± SEM. Data were analyzed by two-tailed Student' s *t*-test

culture supernatant and the results showed that liraglutide significantly inhibited the secretion of CXCL10 by PCOS granulosa cells (Fig. 1E). These results suggest that liraglutide can reduce the level of CXCL10 secreted by PCOS granulosa cells and inhibit the expression of genes associated with inflammation, thereby improving the ovarian microenvironment.

CXCL10 levels were greater in women with PCOS than those in the control group

In our study, 20 women with PCOS and 20 controls were recruited to detect the level of CXCL10 in granulosa cells and follicular fluid. The clinical features are shown in Table 1. No differences were observed in terms of

age, body mass index (BMI) or basal levels of estradiol or follicle stimulating hormone (FSH). Compared with the control women, the women with PCOS had greater LH, testosterone and androstenedione levels ($P<0.05$). Here, we found that *CXCL10* expression was significantly greater in the granulosa cells of the women with PCOS than in those of the control group (Fig. 2A). In addition, the women with PCOS had significantly greater levels of CXCL10 in their follicular fluid than did the control women (Fig. 2B).

Supplementation with CXCL10 impaired mouse follicular growth and ovulation in vitro

To further investigate the effect of CXCL10 on follicle development and ovulation, we used an in vitro follicle culture system and observed that the isolated secondary follicles in the control group gradually grew with antrum formation on Day 6 (Fig. 3A). After 6 days of culture in vitro, the follicle diameter reached approximately 380 μm. However, the follicle growth was inhibited after CXCL10 supplementation, and the diameter of the follicles was approximately 300 μm on Day 6 (Fig. 3B).

For further analysis of the effect of CXCL10 on ovulation, follicles were released from alginate on Day 6 and cultured with hCG for 18 h. After hCG treatment, we observed a rupture of the follicle wall and ovulation of the cumulus-oocyte complex (COC) surrounding the ruptured follicles (Fig. 3C). We also assessed the maturity of follicular oocytes in both groups after hCG treatment.

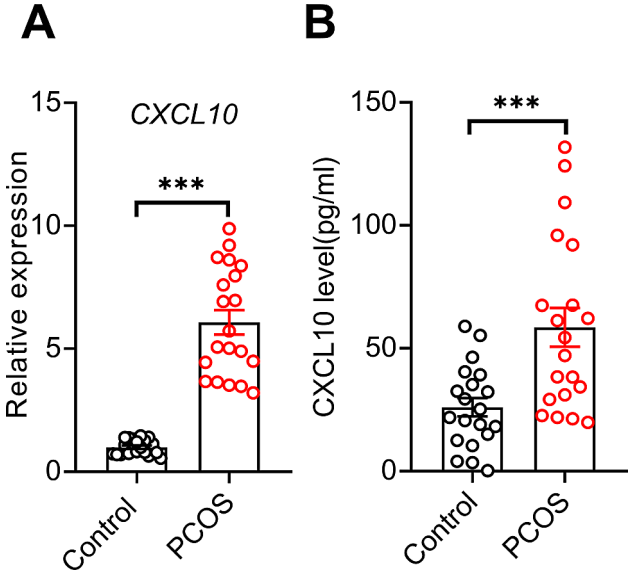

Fig. 2 CXCL10 levels were greater in women with PCOS. (**A**) Changes in *CXCL10* mRNA expression in granulosa cells derived from the control ($n=20$) or PCOS patients ($n=20$). (**B**) CXCL10 levels in the follicular fluid of the control subjects ($n=20$) and the PCOS patients ($n=20$). For (**A**), *P* value was determined by two-tailed Student's t- test. For (**B**), *P* value was determined by a two-tailed Mann–Whitney U test. All the data are presented as the mean ± SEM. ***$P<0.001$

The first polar body in the control group was expelled from the oocyte, indicating that the oocyte had matured, whereas CXCL10 group had fewer oocytes with first polar body extrusion. In addition, the ovulation rate and oocyte maturation rate were significantly reduced in the CXCL10-treated follicles (Fig. 3D&E), and the expression of *Gdf9* and *Bmp15*, which are positively correlated with oocyte maturation, was significantly inhibited by CXCL10 administration (Fig. 3F). In addition, cumulus expansion is crucial for ovulation, and the mRNA levels of the cumulus expansion-related genes *Has2*, *Ptx3*, *Tnfaip6*, *Adamts1* and *Ptgs2* were reduced in the follicles treated with CXCL10 (Fig. 3G). Therefore, CXCL10 inhibited follicle development and ovulation probably through inhibiting oocyte maturation and cumulus expansion.

CXCL10 inhibited follicle development and ovulation by inducing GJA1 overexpressing

Gap junctions between oocytes and surrounding granulosa cells play critical roles in follicle development and ovulation. Recently, Zhang et al. revealed the expression characteristics of gap junction-related genes, including gap junction protein alpha 1 (GJA1), gap junction protein alpha 5 (GJA5), gap junction protein alpha 3 (GJA3) and gap junction protein gamma 1 (GJC1), in human and mouse follicles at different developmental stages [11]. GJA1 and GJA5 were reported to be expressed mainly in granulosa cells, and GJA3 and GJC1 were expressed mainly in oocytes. Interestingly, the expression of GJA1 was downregulated in preovulatory follicles, while GJA5 was expressed mainly in antral follicles and preovulatory follicles.

We found changes in the expression of *Gja1* and *Gja5* in the follicles of the CXCL10-treated group, with *Gja1* upregulated and *Gja5* downregulated (Fig. 4A). Moreover, we observed upregulated *GJA1* and downregulated *GJA5* expression in the granulosa cells of the PCOS patients (Fig. 4B). The same results were observed in mouse granulosa cells (Fig. 4C). *Gja1* was overexpressed after CXCL10 treatment, which was inconsistent with the normal physiological process of decreased *Gja1* expression before ovulation, thus inhibiting follicle development and ovulation. To confirm this finding, we transfected siGja1 into primary mouse granulosa cells, which exhibited significant knockout efficiency at both the RNA (Fig. 4D) and protein (Fig. 4E&F) levels. Results showed a significantly reduced level of Cx43 which was translated by the gene *Gja1*. qPCR revealed that the expression of the cumulus expansion and ovulation-related genes *Ptx3*, *Has2*, *Tnfaip6*, *Adamts1* and *Ptgs2* was inhibited by the administration of CXCL10 to mouse granulosa cells. However, the inhibitory effect of CXCL10 on *Ptx3*, *Has2*, *Tnfaip6* and *Adamts1* gene expression disappeared after

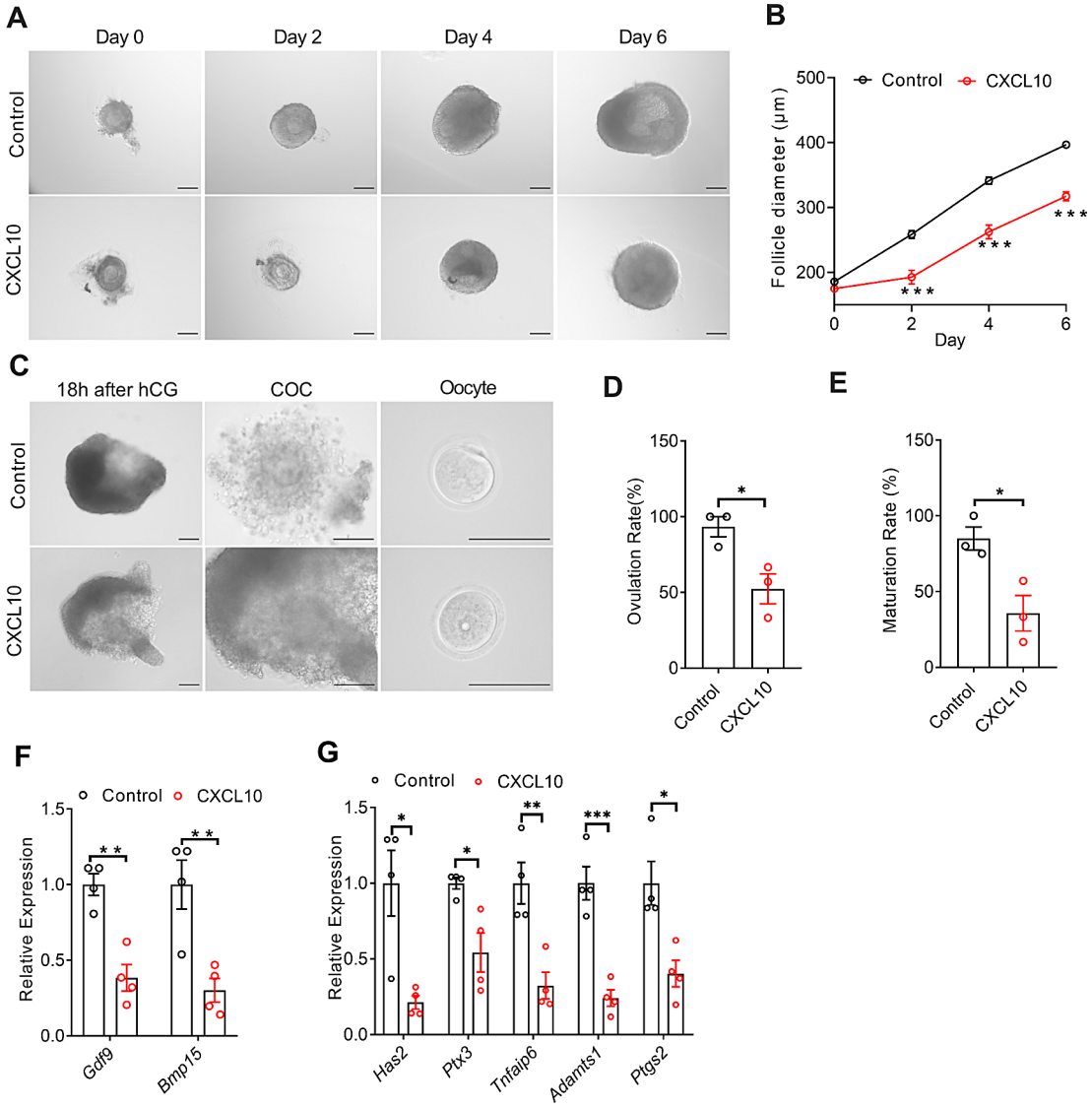

Fig. 3 CXCL10 impaired mouse follicular growth and ovulation in vitro. (**A**) Representative micrograph of mouse follicle culture in vitro. Scale bar: 100 μm. (**B**) Follicle diameters in the control and CXCL10 groups; $n = 11$. (**C**) Representative micrographs of follicles, ovulated COCs and oocytes after 18 h of maturation. Scale bar: 100 μm. (**D**) Ovulation rate of in vitro cultured follicles, $n = 3$. (**E**) Oocyte maturation rate of in vitro cultured follicles, $n = 3$. (**F**) mRNA expression levels of *Gdf9* and *Bmp15* in follicles cultured in vitro; $n = 4$. (G) mRNA expression levels of *Has2*, *Ptx3*, *Tnfaip6*, *Adamts1* and *Ptgs2* in follicles cultured in vitro; $n = 4$. For (Day2 in **B**, **D**, *Ptx3 and Ptgs2* in **G**), *P* values were determined by a two-tailed Mann–Whitney U test. For (Day0, Day4 and Day6 in **B**, **E**-**F**, *Has2*, *Tnfaip6 and Adamts1* in **G**), *P* values were determined by two-tailed Student's t test. All the data are presented as the mean ± SEM. *$P < 0.05$, **$P < 0.01$, ***$P < 0.001$

Gja1 was knocked out (Fig. 4G). The above results suggest that CXCL10 may induce follicular development disorders and ovulatory dysfunction in PCOS patients by affecting the homeostasis of GJA1 between oocyte and granulosa cells before physiological ovulation.

Liraglutide normalized follicular development and ovulation in PCOS by inhibiting CXCL10

For simulating the elevated androgenic environment within PCOS follicles, we treated follicles with DHEA. Our findings indicated that DHEA significantly impedes both follicular growth and the ovulation process. To further explore the specific mechanisms by which liraglutide and CXCL10 affect ovarian function in PCOS patients, we added liraglutide and CXCL10 to DHEA-treated follicles in vitro and observed that, compared to DHEA treatment, supplementation with liraglutide significantly promoted follicular development and follicular cavity formation, while CXCL10 treatment reversed the liraglutide-induced improvement in follicle development (Fig. 5A & B).

To further investigate the effect of liraglutide and CXCL10 on ovulation, we induced in vitro follicular maturation with hCG. After 18 h of hCG

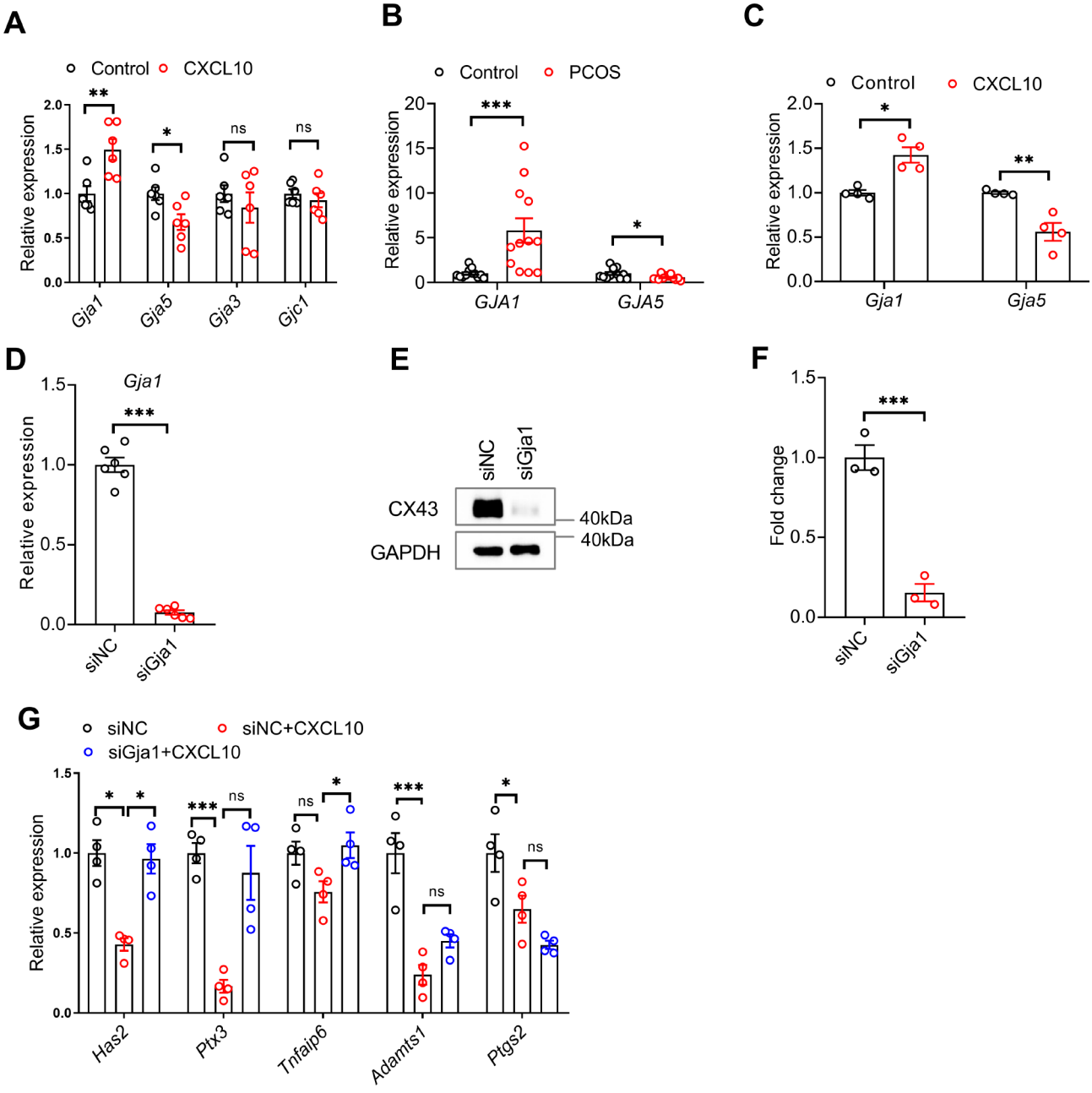

Fig. 4 CXCL10 inhibited follicle development and ovulation by inducing GJA1 overexpressing. (**A**) mRNA expression levels of *Gja1*, *Gja5*, *Gja3* and *Gjc1* in follicles cultured in vitro; $n=6$. (**B**) mRNA expression levels of *GJA1* and *GJA5* in human granulosa cells; $n=12$. (**C**) mRNA expression levels of *Gja1* and *Gja5* in mouse granulosa cells; $n=4$. (**D**) mRNA expression levels of *Gja1* in mouse granulosa cells transfected with siNC or siGja1; $n=6$. (**E**) Representative western blot images of GAPDH and Cx43 in mouse primary granulosa cells transfected with siNC or siGja1. (**F**) The protein expression of Cx43 in mouse granulosa cells transfected with siNC or siGja1 determined via quantitative WB analysis; $n=3$. (**G**) mRNA expression levels of *Has2*, *Ptx3*, *Tnfaip6*, *Adamts1* and *Ptgs2* in mouse primary granulosa cells transfected with siNC, transfected with siNC and incubated with CXCL10, transfected with siGja1 and incubated with CXCL10; $n=4$. For (*GJA1* in **B**), *P* value was determined by a two-tailed Mann–Whitney U test. For (**A**, *GJA5* in **B**, **C**-**D**, **F**), *P* values were determined by two-tailed Student's t test. For (*Tnfaip6*, *Adamts1* and *Ptgs2* in **G**), *P* values were determined by one-way ANOVA with Tukey's multiple comparison post hoc test. For (*Ptx3* in **G**), *P* value was determined by one-way ANOVA with Dunnett's T3 multiple comparison post hoc test. For (*Has2* in **G**), *P* value was determined by Kruskal-Wallis test with Dunn's test. All the data are presented as the mean ± SEM. $^{*}P<0.05$, $^{**}P<0.01$, $^{***}P<0.001$

treatment, ovulation of the accumulated oocyte complex (COC) and mature MII oocytes in the follicles of the DHEA group, DHEA+liraglutide group, and DHEA+liraglutide+CXCL10 group was observed. However, follicles from the DHEA and DHEA+liraglutide+CXCL10 groups did not rupture, while those from the DHEA+liraglutide group ruptured, indicating that liraglutide has a positive effect on ovulation and oocyte

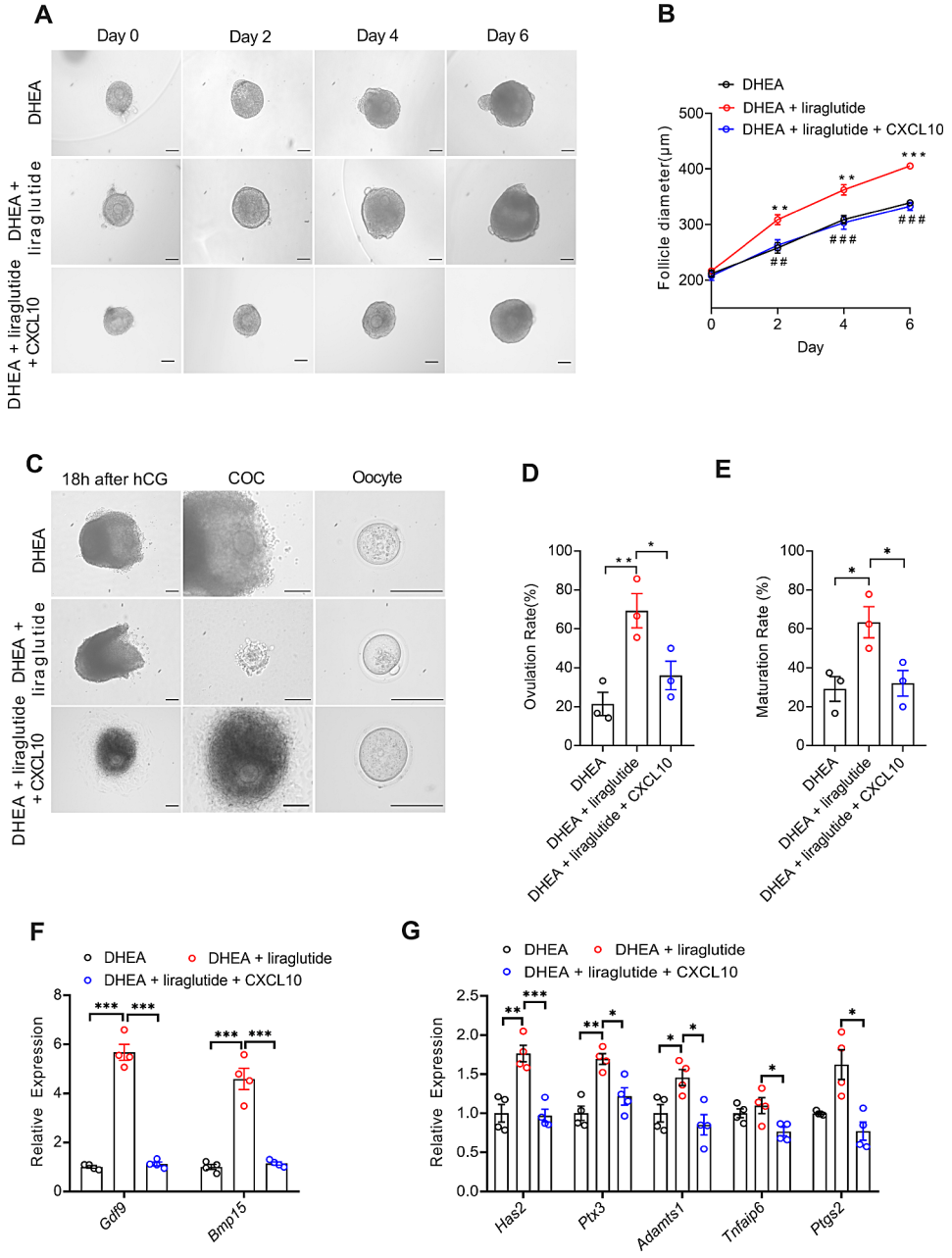

Fig. 5 Liraglutide improved follicular development and ovulation in PCOS by inhibiting CXCL10. (**A**) Representative micrograph of mouse follicles cultured in vitro. Scale bar: 100 μm. (**B**) Follicle diameters in the DHEA, DHEA + liraglutide and DHEA + liraglutide + CXCL10 groups; $n = 11$. * represents the comparison between DHEA group and DHEA + liraglutide group, # represents the comparison between DHEA + liraglutide group and DHEA + liraglutide + CXCL10 group. (**C**) Representative micrographs of follicles, ovulated COCs and oocytes after 18 h of maturation. Scale bar: 100 μm. (**D**) Ovulation rate of in vitro cultured follicles, $n = 3$. (**E**) Oocyte maturation rate of in vitro cultured follicles, $n = 3$. (**F**) mRNA expression levels of *Gdf9* and *Bmp15* in follicles cultured in vitro; $n = 4$. (**G**) mRNA expression levels of *Has2*, *Ptx3*, *Tnfaip6*, *Adamts1* and *Ptgs2* in follicles cultured in vitro; $n = 4$. For (Day2, Day4 in **B**, **D**, **E**), *P* values were determined by one-way ANOVA with Tukey's multiple comparison post hoc test. For (Day0, Day6 in **B**, *Tnfaip6* in **G**), the *P* values were determined by the Kruskal–Wallis test followed by Dunn's post hoc test. For (**F**, *Has2*, *Ptx3*, *Adamts1*, *Ptgs2* in **G**), *P* values were determined by one-way ANOVA with Dunnett's T3 multiple comparison post hoc test. All the data are presented as the mean ± SEM. $^{*}P < 0.05$, $^{**}P < 0.01$, $^{***}P < 0.001$, $^{\#\#}P < 0.01$, $^{\#\#\#}P < 0.001$

maturation (Fig. 5C). Specifically, liraglutide inhibited CXCL10. These findings were further confirmed by the statistical analysis of the ovulation and oocyte maturation rates (Fig. 5D&E). The results showed that, compared with that in the DHEA group, the expression of *Gdf9* and *Bmp15* was significantly greater in the DHEA + liraglutide group, while CXCL10 supplementation inhibited the expression of these genes. In addition,

DHEA+liraglutide significantly increased the expression of *Has2*, *Ptx3* and *Adamts1*, while DHEA+liraglutide+CXCL10 significantly inhibited the expression of *Has2*, *Ptx3*, *Tnfaip6*, *Adamts1* and *Ptgs2* (Fig. 5F&G). The above results suggest that liraglutide may promote ovulation by enhancing oocyte maturation and cumulus expansion via the inhibition of CXCL10.

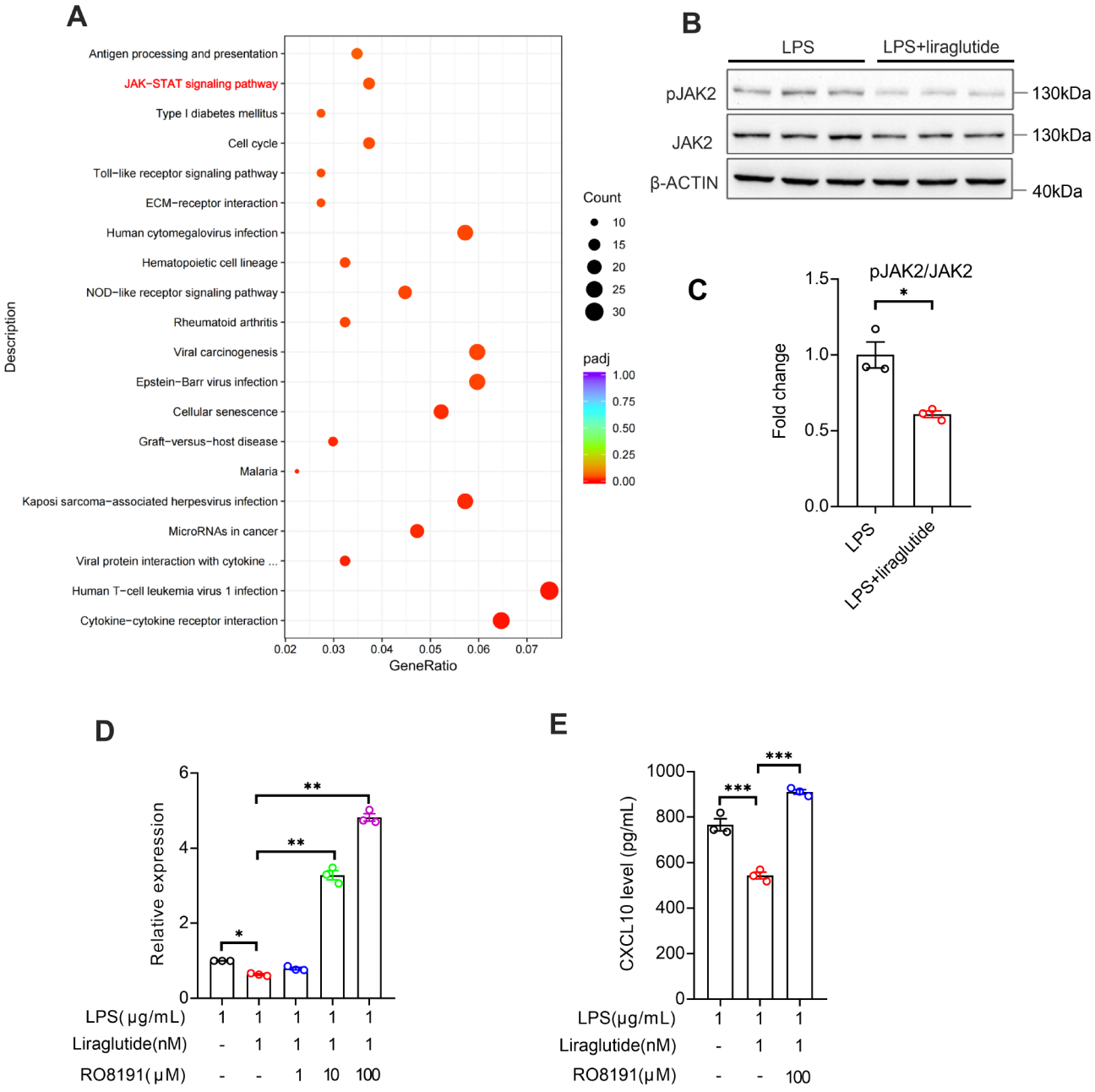

Fig. 6 Liraglutide inhibited the secretion of CXCL10 in granulosa cells by disrupting the JAK signaling pathway. (**A**) KEGG pathway analysis showing the top 20 pathways enriched in PCOS + Liraglutide versus PCOS group. (**B**) Representative western blot images of β-ACTIN, JAK2 and pJAK2 in KGN cells. (**C**) The ratio of the protein expression of pJAK2 and JAK2 in KGN cells treated with LPS and LPS + liraglutide determined via quantitative WB analysis; $n = 3$. (**D**) mRNA expression levels of *CXCL10* in KGN cells incubated with LPS, liraglutide or RO8191 for 24 h; $n = 3$. (**E**) CXCL10 levels in the cell culture supernatant after incubation with LPS, liraglutide or RO8191 for 24 h in KGN cells; $n = 3$. For (**C**), *P* value was determined by two-tailed Student's t test. For (**D**), *P* values were determined by one-way ANOVA with Dunnett's T3 multiple comparison post hoc test. For (**E**), *P* values were determined by one-way ANOVA with Tukey's multiple comparison post hoc test. All the data are presented as the mean ± SEM. *$P < 0.05$, **$P < 0.01$, ***$P < 0.001$

Liraglutide inhibited the secretion of CXCL10 in granulosa cells by inhibiting the JAK signaling pathway

To explore how liraglutide inhibits CXCL10 secretion in granulosa cells, we performed KEGG analysis of the DEGs, in which the JAK-STAT signaling pathway was significantly enriched (Fig. 6A). The JAK signaling pathway regulates multiple cellular mechanisms associated with the development of various diseases. To evaluate the role of JAK signaling in the regulation of CXCL10 expression, we activated the inflammatory state in KGN cells using LPS. KGN cells, derived from human granulosa cell tumors, exhibit most of the physiological activities and functions of normal granulosa cells, and were used here for mechanistic exploration experiments. Western blotting confirmed that liraglutide reduced the ratio of phosphorylated JAK2 to JAK2 (Fig. 6B&C). In addition, we used LPS to activate the inflammatory state in KGN cells and found that liraglutide reduced CXCL10 expression. Moreover, cells were treated with different concentrations of RO8191 (interferon receptor agonist and JAK signaling pathway activator), and 1 μM, 10 μM, and 100 μM RO8191 improved the expression of *CXCL10*; the effect became more pronounced with increasing concentration (Fig. 6D). In addition, we detected CXCL10 levels in the supernatants of the cells treated with LPS, liraglutide or RO8191 (100 μM) and found that liraglutide could reduce CXCL10 levels, while RO8191 could increase CXCL10 levels (Fig. 6E). These results indicate that activation of the JAK signaling pathway can increase CXCL10 secretion in granulosa cells and that liraglutide inhibits CXCL10 secretion in granulosa cells by inhibiting the JAK-STAT pathway.

Discussion

To validate the effect of liraglutide, we treated PCOS granulosa cells with liraglutide and found that liraglutide treatment significantly inhibit the expression of classic inflammatory factors including *CXCL10*, *IL-1B* and *IL-6*, indicating that liraglutide may act as an effective anti-inflammatory factor in PCOS. Due to the important role of local inflammation in follicle development and ovulation, we measured the levels of CXCL10 in the follicular fluid of the control and PCOS patients and found that follicular CXCL10 levels were significantly increased in the women with PCOS. In addition, supplementation with CXCL10 inhibited follicle growth and ultimately impaired the ovulation process by elevating GJA1 expression and disrupting the homeostasis of GJA1 between oocyte and granulosa cells before physiological ovulation. Furthermore, liraglutide, a regulator of inflammatory factors, evidently improved DHEA-induced aberrant follicle development and ovulatory dysfunction, which was disrupted by CXCL10 supplementation. Many studies have revealed that liraglutide inhibits CXCL10 secretion from PCOS-affected granulosa cells by blocking JAK-STAT signaling pathways. Overall, this study investigated the impact of CXCL10 on follicle development and ovulation and further explored the therapeutic effect of liraglutide on follicle development and ovulation in PCOS via the inhibition of CXCL10 secretion, which provides additional evidence for the application of liraglutide in PCOS treatment.

GLP-1 can achieve protective effects on metabolic diseases through multiple pathways. In addition to its direct effect, anti-inflammation is also an important part of GLP-1's effect to improve metabolic abnormalities. GLP-1 can not only suppress inflammation by acting on immune cells, but also reduce the levels of inflammatory factors in the circulation and local tissue, thereby improving the inflammatory state [12]. Studies have shown that the GLP-1 analog exendin-4 can improve type 1 diabetes by reducing local CXCL10 levels in pancreatic islet tissue [13]. Liraglutide is a GLP-1 receptor agonist and can significantly reduce body weight and improve metabolism. Additionally, its therapeutic effect on PCOS has received widespread attention [14, 15], but the specific molecular mechanism remains to be explored. This study found that liraglutide can improve DHEA-induced follicular development abnormalities and ovulation disorders, while inhibiting follicular CXCL10 gene expression. Adding CXCL10 blocks the effect of liraglutide. Mechanism study results show that liraglutide may inhibit the secretion of CXCL10 by granulosa cells by inhibiting JAK2 phosphorylation, improve local inflammation in the ovaries, thereby improving abnormal follicular development and ovulation disorders in PCOS.

As a proinflammatory chemokine, CXCL10 is extensively correlated with the development of various conditions, including infectious diseases, autoimmune diseases, tumorigenesis and metabolic disorders. Currently, metabolic disorders are widespread in the population, and the impairment of reproductive function by metabolic dysfunction has also attracted increased interest. In the adipose tissue of obese humans and mice, activated T-bet$^+$ B cells were reported to accumulate and secrete CXCL10, which exacerbates obesity-associated metabolic abnormalities. Additionally, Ruebel et al. revealed that obesity is associated with ovarian inflammation, enhancement of the chemokine signaling pathway and increased expression of CXCL10 in the ovarian tissue of obese dams. In addition, the ovarian expression of glucose transporter (GLUT) 4 and GLUT9 was significantly decreased in obese mice, which seems to be correlated with ovarian inflammation [16]. Thus, CXCL10 is closely related to the development of metabolic disorders. Approximately 37-39% of PCOS patients exhibit metabolic syndrome, which is characterized by high BMI and insulin resistance, indicating the possible role of

CXCL10 in PCOS pathogenesis. Moreover, female rhesus macaques that received testosterone implants exhibited significantly increased follicular CXCL10 levels [17]. In this study, we found that the level of CXCL10 in the follicular fluid of the PCOS patients was evidently greater than that in the follicular fluid of the BMI-matched control women, indicating that CXCL10 may contribute to PCOS development in multiple ways.

Some researchers believe that under normal physiological conditions, an increase in local cytokine secretion and immune cell infiltration in the ovaries can promote ovulation. According to previous reports, the concentration of CXCL10 in follicular fluid increases 6–8 times after 2 h of ovulation [18], indicating a close correlation between the peak CXCL10 concentration and ovulation. However, in the ovaries of PCOS patients, CXCL10 levels remain consistently high, and in vitro experiments have shown that CXCL10 treatment can significantly inhibit follicular development and ovulation, suggesting that CXCL10 is involved in the abnormal follicle development and ovulation in women with PCOS. However, the specific mechanism may be complex. CXCL10 administration reportedly decreased the mRNA levels of FSHR and CYP19A1 in human granulosa cells in vitro [19]. Other studies have shown that CXCL10 has no effect on hormone secretion or other functions of ovarian granulosa cells and that CXCL10 affects follicle development by promoting collagen deposition [20]. Therefore, CXCL10 may affect follicular development by reshaping the ovarian microenvironment.

Bidirectional communication between oocytes and surrounding granulosa cells occurs throughout the process of follicle development. Gap junctions play an important role in the crosstalk between two cell types; granulosa cells meet the metabolic needs of oocytes, and oocytes prevent corpus luteum formation from granulosa cells [21, 22]. As the main protein of gap junctions intercellular communication (GJIC), connexin is involved in material exchange and signal transmission between oocytes and granulosa cells. Gap junction channels allow ions, small molecule metabolites and second messengers and so on to pass through, thus participating in physiological processes such as follicle development and ovulation. Cx43, also written as GJA1, plays a critical role in ovarian folliculogenesis and ovulation [23, 24]. In addition, GJA5 expression is considered an essential factor required for oocyte maturation [25]. According to the transcriptome landscape of human folliculogenesis, Zhang et al. analyzed the expression patterns of connexin-encoding genes in human follicles at different stages. The expression of connexin in follicles is a dynamic process. GJA1 was expressed in granulosa cells throughout all the follicular stages. Specifically, GJA1 expression is reduced during the periovulation period, which contributes to the resumption of meiosis and the initiation of the ovulation process. In contrast, GJA5 was preferentially expressed in granulosa cells of antral and preovulatory follicles [26]. The growth and development of follicles and ovulation are closely related to gonadotropins, and it has been reported that FSH and LH affect the GJIC of granulosa cells in a stage-specific manner. FSH promotes an increase in Cx43 during the sinus follicular phase, while LH down-regulates Cx43 levels, which may explain why GJA1 expression is down-regulated in preovulation follicles [27, 28] and this is consistent with the conclusion of Zhang et al. However, there was another view that abnormal expression of GJA1 in granulosa cells could be involved in oocyte meiotic resumption and ovulatory disorders [29, 30], which may contribute to reproductive dysfunction. In addition to Cx43, it was also reported that Cx26 expression was down-regulated in bovine ovaries collected at 10, 20 and 25 h after gonadotropin-releasing hormone (GnRH) injection [31]. In summary, the expression level of a single connexin may not fully represent the functional strength of the overall gap junction, and the influence on ovulation needs to be comprehensively analyzed according to the specific stage of follicle development and specific connexin. To date, a definitive consensus on the correlation between gap junction intensity and ovulation has not been established. Integrating the findings of this study with those of previous research, we believe that any homeostasis disturbance of Cx43 levels associated with physiological ovulation may affect ovulation. This effect could potentially be linked to the intricate interplay and dynamic fluctuations of various gap junction proteins that occur during the ovulatory process. However, this hypothesis requires further investigation and validation.

To further explore the mechanism by which CXCL10 inhibits follicle development in PCOS patients, we investigated the impact of CXCL10 on gap junctions between oocytes and granulosa cells and found that after hCG administration, the expression of GJA1 was significantly increased, while GJA5 expression was inhibited in CXCL10-treated follicles; moreover, CXCL10 had little impact on the expression of GJA3 and GJC1, both of which are expressed in oocytes. Target depletion of GJA1 significantly inhibited ovulation-related gene expression in vitro, validating the important role of GJA1 in the ovulation process. Furthermore, CXCL10-mediated inhibition of ovulation-related gene expression was reversed by GJA1 depletion in granulosa cells, suggesting that CXCL10 acts by aberrantly elevating GJA1 expression and disrupting the homeostasis of GJA1 between oocyte and granulosa cells before physiological ovulation, thus inhibiting follicle development and ovulation.

Conclusion

In summary, we demonstrated liraglutide significantly inhibit ovarian inflammation in PCOS ovaries, and aberrantly increased follicular CXCL10 levels significantly impaired follicle development in women with PCOS. In addition, supplementation with CXCL10 inhibited follicle growth and ultimately impaired the ovulation process by inducing GJA1 overexpression. Furthermore, we demonstrated the therapeutic effect of liraglutide on PCOS through the inhibition of JAK2 phosphorylation and CXCL10 secretion in granulosa cells. Our results provide supportive evidence for the application of liraglutide in treating PCOS, especially in inhibiting local inflammation in ovarian tissue and improving the ovarian microenvironment, thus providing new insights into the treatment of abnormal follicle development and ovulatory disorders in patients with PCOS.

Materials and methods

Human subjects

The study was approved by the Ethics Committee of Peking University Third Hospital according to the Council for International Organizations of Medical Sciences. All participants signed informed consent documents before participation in the study.

We recruited 28 individuals with PCOS and 20 controls of Chinese ancestry from the Reproductive Medical Center at Peking University Third Hospital from December 2022 to May 2024. After we excluded subjects with other conditions that might cause hyperandrogenemia or ovulatory dysfunction (Cushing syndrome, 21-hydroxylase deficiency, thyroid disease, androgen-secreting tumors, congenital adrenal hyperplasia and hyperprolactinemia), women with PCOS were diagnosed according to the 2003 Rotterdam criteria, which require the presence of at least two of the following conditions: (1) oligo-ovulation and/or anovulation; (2) clinical and/or biochemical signs of hyperandrogenism; and (3) polycystic ovaries.

Follicular fluid and granulosa cell collection and culture

As described previously [32], we collected grossly clear follicular fluid and ovarian granulosa cells from all participants. Human granulosa cells were cultured in DMEM-F12 supplemented with 10% fetal bovine serum (FBS; Gibco) and 1% penicillin–streptomycin (PS; 5,000 U/mL; Gibco) for 12 h. A portion of the granulosa cells from PCOS patients was incubated with liraglutide (500 ng/ml; PeproTech) for 24 h, and the remaining cells were cultured in basal culture medium and subsequently collected for RNA extraction. We also collected cell culture supernatants to detect CXCL10 levels.

Mouse granulosa cell collection and culture

Primary mouse granulosa cells were obtained from 6- to 8-week-old C57BL/6J female mice. Mice were intraperitoneally injected with 5–10 IU of pregnant mare serum gonadotropin (PMSG; Ningbo, China). After 46–48 h, the ovaries were removed, and granulosa cells were separated via micro forceps and an insulin injection needle. Granulosa cells were collected with a mouth pipette, washed with DPBS, cultured in DMEM-F12 supplemented with 10% FBS and 1% PS (5,000 U/mL) for 24 h, and subsequently transferred for RNA extraction and protein extraction.

KGN cell culture

A granulosa cell tumor-derived cell line (KGN) was utilized to explore the ability of liraglutide to regulate CXCL10. KGN cells were seeded in six-well plates in DMEM/F12 culture medium supplemented with 10% fetal bovine serum and 1% penicillin–streptomycin (5,000 U/mL) as well as LPS (1 μg/mL; Solarbio), liraglutide (1 nM; Novo Nordisk) and RO8191 (1 μM, 10 μM, 100 μM; MedChemExpress).

In vitro culture and maturation of mouse ovarian follicles

We used 18- to 21-day-old C57BL/6J female mouse ovaries to mechanically separate healthy secondary follicles with a diameter of 180–200 μm. The separated follicles were incubated in αMEM (32571036, Sigma–Aldrich) supplemented with 1% FBS for 1 h, encapsulated with 0.5% alginate (Sigma–Aldrich) and cultured in 96-well plates with αMEM supplemented with 3 mg/ml BSA (B2064, Sigma–Aldrich), 1 mg/ml bovine fetuin (F2379, Sigma–Aldrich), 10 mIU/ml recombinant follicle stimulating hormone, 5 μg/ml insulin, 5 μg/ml transferrin, and 5 μg/ml selenium (I3146, Sigma–Aldrich) for 6 days. DHEA (0.01 mM; HY-14650; MedChemExpress), liraglutide (1 nM; Novo Nordisk) or CXCL10 (0.01 mM; PeproTech) was added to the growth media. Half of the growth media was changed every 2 days, and the follicles were imaged by fluorescence microscopy after each medium change.

For in vitro maturation, follicles were released from alginate beads and incubated in αMEM supplemented with 10% FBS, 1% PS, 1.5 IU/ml human chorionic gonadotropin (hCG), and 10 ng/ml epidermal growth factor (EGF, PHG0311, Gibco) for 18 h. After 18 h of hCG treatment, follicles, COCs and oocytes were imaged. The oocyte that released the first polar body was mature. The ovulation rate and maturation rate were calculated by observing the ovulation of five to nine follicles each time, experiments were repeated three times for statistical analysis. Every 3 follicles were collected for RNA extraction.

RNA extraction and RNA sequencing (RNA-seq) analysis

Total RNA was extracted from granulosa cells with TRIzol reagent (15596018; Life Technologies), and total RNA was extracted from follicles with a RNeasy Mini Kit (74104; QIAGEN) according to the manufacturer's protocol. The total RNA concentration was measured with a NanoDrop 2000 C spectrophotometer. Total RNA (1000 ng or 2000 ng) was used to synthesize cDNA. Granulosa cells collected from follicular fluid of PCOS patients were treated with or without liraglutide and then RNA extracted for RNA-seq analysis. Following the manufacturer's recommendations, sequencing libraries were generated from a total of 1 mg RNA per sample, which had been quantified and qualified, using the NEBNext® UltraTM RNA Library Prep Kit for Illumina® (NEB, USA). Index codes were incorporated to assign sequences to each sample. The index-coded samples were then clustered on a cBot Cluster Generation System with the TruSeq PE Cluster Kit v3-cBot-HS (Illumina), as per the manufacturer's instructions. Subsequently, the library preparations were sequenced on an Illumina Novaseq platform to produce 150 bp paired-end reads. Prior to data analysis, raw data in fastq format underwent quality control through in-house perl scripts, resulting in clean data (clean reads) by excluding reads with adapters, poly-N, and low-quality reads. Concurrently, the Q20, Q30, and GC content of the clean data were determined. All subsequent analyses were conducted using these high-quality clean data. Reference genome and gene model annotation files were directly downloaded from a genome website. The reference genome index was constructed using Hisat2 v2.0.5, and paired-end clean reads were aligned to the reference genome with the same tool. Genes were considered significantly differentially expressed if they met the criteria of FDR $P<0.05$ and log2 fold change>1. Bioinformatic analysis was carried out using the OmicStudio tools available at https://www.omicstudio.cn/tool.

Table 2 Primer sequences for real-time PCR used in the study

Target genes	Primer sequences
18s(mouse)	forward 5′-CGGCTACCACATCCAAGGAA-3′
	forward 5′-CGGCTACCACATCCAAGGAA-3′
Gdf9(mouse)	forward 5′-TCTTAGTAGCCTTAGCTCTCAGG-3′
	reverse 5′-TGTCAGTCCCATCTACAGGCA-3′
Bmp15(mouse)	forward 5′-TCCTTGCTGACGACCCTACAT-3′
	reverse 5′-TACCTCAGGGGATAGCCTTGG-3′
Has2(mouse)	forward 5′-TGTGAGAGGTTTCTATGTGTCCT-3′
	reverse 5′-ACCGTACAGTCCAAATGAGAAGT-3′
Ptx3(mouse)	forward 5′-CCTGCGATCCTGCTTTGTG-3′
	reverse 5′-GGTGGGATGAAGTCCATTGTC-3′
Tnfaip6(mouse)	forward 5′-GGGATTCAAGAACGGGATCTTT-3′
	reverse 5′-TCAAATTCACATACGGCCTTGG-3′
Adamts1(mouse)	forward 5′-CATAACAATGCTGCTATGTGCG-3′
	reverse 5′-TGTCCGGCTGCAACTTCAG-3′
Ptgs2(mouse)	forward5′-TGAGCAACTATTCCAAACCAGC-3′
	reverse 5′-GCACGTAGTCTTCGATCACTATC-3′
Cxcl10(mouse)	forward 5′-GGTCTGAGTCCTCGCTCAAG-3′
	reverse 5′-GTCGCACCTCCACATAGCTT-3′
Gja1(mouse)	forward 5′-CATTAAGTGAAAGAGAGGTGC-3′
	reverse 5′-GGAGCAGGATTCTGAAAATG-3′
Gja5(mouse)	forward 5′-TGAGCTCTAAACGTGGAAGGC-3′
	reverse 5′-ATGGTATCGCACCGGAAGTC-3′
Gja3(mouse)	forward 5′-CCGCACGAGTAAAGAGGGAG-3′
	reverse 5′-GCTGTGTGTTGCAGGTGAAG-3′
Gjc1(mouse)	forward 5′-GCAGACTTCCTTGCCCTCAT-3′
	reverse 5′-ACCATGGGGGTTGTTTTGGT-3′
GJA1(human)	forward 5′-CAGCCACTAGCCATTGTGGA-3′
	reverse 5′-GGCTGTTGAGTACCACCTCC-3′
GJA5(human)	forward 5′-AGAGTGTGAAGAAGCCCACG-3′
	reverse 5′-AGGCTAAGGAGGAGGGACAG-3′
CXCL10(human)	forward 5′-GCTTCCAAGGATGGACCACA-3′
	reverse 5′-GCAGGGTCAGAACATCCACT-3′
CXCL9(human)	forward 5′-CCAGTAGTGAGAAAGGGTCGC-3′
	reverse 5′- AGGGCTTGGGGCAAATTGTT-3′
CXCL8(human)	forward 5′- ATGACTTCCAAGCTGGCCGTGGCT-3′
	reverse 5′- TCTCAGCCCTCTTCAAAAACTTCTC-3′
IL1B(human)	forward 5′- ATGATGGCTTATTACAGTGGCAA-3′
	reverse 5′- GTCGGAGATTCGTAGCTGGA-3′
IL1A(human)	forward 5′-TGGTAGTAGCAACCAACGGGA-3′
	reverse 5′- ACTTTGATTGAGGGCGTCATTC-3′
CSF2(human)	forward 5′- TCCTGAACCTGAGTAGAGACAC-3′
	reverse 5′- TGCTGCTTGTAGTGGCTGG-3′
TNFSF10(human)	forward 5′- TGCGTGCTGATCGTGATCTTC-3′
	reverse 5′- GCTCGTTGGTAAAGTACACGTA-3′
IFNAR2(human)	forward 5′- TCATGGTGTATATCAGCCTCGT-3′
	reverse 5′- AGTTGGTACAATGGAGTGGTTTT-3′
IL6(human)	forward 5′-CCTGAACCTTCCAAAGATGGC-3′
	reverse 5′-TTCACCAGGCAAGTCTCCTCA-3′

Real-time quantitative PCR (qPCR) analysis

Real-time qPCR analysis was performed using SYBR Green PCR master mix (Invitrogen) and an ABI 7500 real-time PCR system (Applied Biosystems). The qPCR primers used in this study can be found in Table 2. All qPCRs were carried out in a final volume of 20 µl following the manufacturer's instructions (Invitrogen). The amplification thermal cycling conditions were as follows: 95 °C for 2 min, 40 cycles at 95 °C for 15 s and 60 °C for 40 s.

Transfection of siRNA

Lipofectamine RNAiMAX was used to transfect siRNAs into mouse primary granulosa cells according to the manufacturer's instructions (13778-150, Invitrogen). All siRNAs were obtained from Sangon Biotech (Shanghai, China). The sequences of siGja1 were as follows: 5′-CUC UCGCUCUGAAUAUCAUTT-3′ (sense) and 5′-AUGAU

AUUCAGAGCGAGAGTT-3' (antisense). The sequences of the nontargeting control siRNAs (siNCs) used were as follows: 5'-UUCUCCGAACGUGUCACGUTT-3' (sense) and 5'-ACGUGACACGUUCGGAGAATT-3' (antisense). We used quantitative real-time RT–PCR and western blot analysis to evaluate the knockdown efficiency of the target siRNA. We collected other mouse primary granulosa cells for RNA extraction.

Western blot analysis

After treatment, human and mouse granulosa cells were lysed in RIPA lysis buffer containing PMSF (Applygen, China), and the protein concentration was determined using a Pierce™ BCA protein assay according to the manufacturer's instructions (Thermo Scientific, USA). Equal amounts of protein were loaded and separated using sodium dodecyl sulfate–polyacrylamide gel electrophoresis (SDS–PAGE) and then transferred onto polyvinylidene difluoride (PVDF) membranes (PALL, USA). The PVDF membranes were blocked with 5% skim milk at room temperature for one hour and then incubated with the primary antibodies mouse anti-JAK2 (1:1000; 3230; Cell Signaling Technology), rabbit anti-pJAK2 (1:1000; 3771; Cell Signaling Technology), rabbit anti-CX43 (1:1000; A11752; ABclonal), rabbit anti-GAPDH (1:1000; 5174; Cell Signaling Technology) and rabbit anti-β-ACTIN (1:10000; AC038; ABclonal). The next day, the membranes were washed with TBST and then incubated with the appropriate HRP-conjugated secondary antibody for one hour at room temperature. Finally, the immunoreactive bands were detected with Pierce™ ECL Western Blotting Substrate (Thermo Scientific, USA). The intensities of the bands were quantified with ImageJ software and normalized to that of β-ACTIN.

Statistical analysis

GraphPad Prism version 8.0 (GraphPad Software) and SPSS version 24.0 were used for statistical analysis. The sample distribution was determined by the Kolmogorov–Smirnov normality test. For parametric data, a two-tailed Student's t test was used to evaluate the statistical significance of differences between two groups, and one-way analysis of variance (ANOVA) followed by Tukey's post hoc test or Dunnett's T3 post was used to evaluate the statistical significance of differences among three or more groups. For nonparametric data, the two-tailed Mann–Whitney U test was used to evaluate statistical significance of differences between two groups, and the Kruskal–Wallis test followed by Dunn's post hoc test was used to evaluate the statistical significance of differences among three or more groups. The data are shown as the mean ± SEM. $P<0.05$ was considered to indicate statistical significance. $^{*}P<0.05$, $^{**}P<0.01$, $^{***}P<0.001$.

Abbreviations

PCOS	Polycystic ovary syndrome
GLP-1	Glucagon-like peptide-1
CXCL10	C-X-C motif chemokine ligand 10
TZPs	Transzonal projections
TBT	Tributyltin
LH	Luteinizing hormone
TNF-α	Tumor necrosis factorα
IL-18	Interleukin 18
IL-6	Interleukin 6
BMI	Body mass index
FSH	Follicle stimulating hormone
COC	Cumulus-oocyte-complex
GJA1	Gap junction protein alpha 1
GJA5	Gap junction protein alpha 5
GJA3	Gap junction protein alpha 3
GJC1	Gap junction protein gamma 1
Cx43	Connexin 43
DEGs	Differentially expressed genes
PS	Penicillin-streptomycin

Supplementary Information

The online version contains supplementary material available at https://doi.org/10.1186/s12958-024-01269-9.

Supplementary Material 1

Acknowledgements

Not applicable.

Author contributions

M.Z. and B.L. performed the experiments and drafted the manuscript. B.L. and C.Y. conducted the bioinformatics analyses. X.Q. and C.Y. helped with the data analysis and manuscript revision. Y.P. conceived and designed the research and approved the final version of the manuscript. All the authors contributed to the article and approved the submitted version.

Funding

This work was supported by the National Natural Science Foundation of China (82371643, 82288102, 82171627).

Data availability

No datasets were generated or analysed during the current study.

Declarations

Ethics approval and consent to participate

This work involving human participants was reviewed and approved by the Peking University Third Hospital Medical Science Research Ethics Committee. The patients/participants provided their written informed consent to participate in this study. The animal study was reviewed and approved by the Animal Care and Use Committee of Peking University.

Consent for publication

Not applicable.

Competing interests

The authors declare no competing interests.

Author details

[1]State Key Laboratory of Female Fertility Promotion, Center for Reproductive Medicine, Department of Obstetrics and Gynecology, Peking University Third Hospital, Beijing, China
[2]National Clinical Research Center for Obstetrics and Gynecology (Peking University Third Hospital), Beijing, China
[3]Key Laboratory of Assisted Reproduction (Peking University), Ministry of Education, Beijing, China

[4]Beijing Key Laboratory of Reproductive Endocrinology and Assisted Reproductive Technology, Beijing, China
[5]Institute of Advanced Clinical Medicine, Peking University, Beijing, China

Received: 12 February 2024 / Accepted: 25 July 2024
Published online: 06 August 2024

References

1. Bozdag G, et al. The prevalence and phenotypic features of polycystic ovary syndrome: a systematic review and meta-analysis. Hum Reprod. 2016;31(12):2841–55.
2. Teede HJ, et al. Recommendations from the 2023 International evidence-based Guideline for the Assessment and Management of Polycystic Ovary Syndrome. Fertil Steril. 2023;120(4):767–93.
3. Azziz R, et al. Polycystic ovary syndrome. Nat Rev Dis Primers. 2016;2:16057.
4. Gilchrist RB, Lane M, Thompson JG. Oocyte-secreted factors: regulators of cumulus cell function and oocyte quality. Hum Reprod Update. 2008;14(2):159–77.
5. Jaffe LA, Egbert JR. Regulation of mammalian oocyte meiosis by Intercellular Communication within the ovarian follicle. Annu Rev Physiol. 2017;79:237–60.
6. Chen M, et al. Resveratrol ameliorates polycystic ovary syndrome via transzonal projections within oocyte-granulosa cell communication. Theranostics. 2022;12(2):782–95.
7. Ratchford AM, Esguerra CR, Moley KH. Decreased oocyte-granulosa cell gap junction communication and connexin expression in a type 1 diabetic mouse model. Mol Endocrinol. 2008;22(12):2643–54.
8. Oakley OR, et al. Periovulatory leukocyte infiltration in the rat ovary. Endocrinology. 2010;151(9):4551–9.
9. Brannstrom M, Mayrhofer G, Robertson SA. Localization of leukocyte subsets in the rat ovary during the periovulatory period. Biol Reprod. 1993;48(2):277–86.
10. Escobar-Morreale HF, Luque-Ramirez M, Gonzalez F. Circulating inflammatory markers in polycystic ovary syndrome: a systematic review and metaanalysis. Fertil Steril. 2011;95(3):1048–e581.
11. Zhang Y, et al. Transcriptome Landscape of Human Folliculogenesis reveals oocyte and Granulosa Cell interactions. Mol Cell. 2018;72(6):1021–e10344.
12. Bendotti G, et al. The anti-inflammatory and immunological properties of GLP-1 receptor agonists. Pharmacol Res. 2022;182:106320.
13. Pugazhenthi U, et al. Anti-inflammatory action of exendin-4 in human islets is enhanced by phosphodiesterase inhibitors: potential therapeutic benefits in diabetic patients. Diabetologia. 2010;53(11):2357–68.
14. Elkind-Hirsch KE, et al. Liraglutide 3 mg on weight, body composition, and hormonal and metabolic parameters in women with obesity and polycystic ovary syndrome: a randomized placebo-controlled-phase 3 study. Fertil Steril. 2022;118(2):371–81.
15. Salamun V, et al. Liraglutide increases IVF pregnancy rates in obese PCOS women with poor response to first-line reproductive treatments: a pilot randomized study. Eur J Endocrinol. 2018;179(1):1–11.
16. Ruebel M, et al. Maternal obesity is associated with ovarian inflammation and upregulation of early growth response factor 1. Am J Physiol Endocrinol Metab. 2016;311(1):E269–77.
17. Ravisankar S et al. Long-term hyperandrogenemia and/or western-style Diet in Rhesus Macaque females impairs preimplantation embryogenesis. Endocrinology, 2022. 163(4).
18. Abdulrahman Alrabiah N, et al. Immunological aspects of ovarian follicle ovulation and corpus luteum formation in cattle. Reproduction. 2021;162(3):209–25.
19. Han MT, et al. The cytokine profiles in follicular fluid and reproductive outcomes in women with endometriosis. Am J Reprod Immunol. 2023;89(6):e13633.
20. Wang C, Sun Y. Induction of Collagen I by CXCL10 in ovarian Theca-Stroma cells via the JNK pathway. Front Endocrinol (Lausanne). 2022;13:823740.
21. Buccione R, Schroeder AC, Eppig JJ. Interactions between somatic cells and germ cells throughout mammalian oogenesis. Biol Reprod. 1990;43(4):543–7.
22. Simon AM, et al. Female infertility in mice lacking connexin 37. Nature. 1997;385(6616):525–9.
23. Ackert CL, et al. Intercellular communication via connexin43 gap junctions is required for ovarian folliculogenesis in the mouse. Dev Biol. 2001;233(2):258–70.
24. Juneja SC, et al. Defects in the germ line and gonads of mice lacking connexin43. Biol Reprod. 1999;60(5):1263–70.
25. Song HJ, et al. Influence of epidermal growth factor supplementation during in vitro maturation on nuclear status and gene expression of canine oocytes. Res Vet Sci. 2011;91(3):439–45.
26. Zhang Y, et al. Transcriptome Landscape of Human Folliculogenesis reveals oocyte and Granulosa Cell interactions. Mol Cell. 2018;72(6):1021–34. e4.
27. Sommersberg B, et al. Gap junction communication and connexin 43 gene expression in a rat granulosa cell line:: regulation by follicle-stimulating hormone. Biol Reprod. 2000;63(6):1661–8.
28. Kalma Y, et al. Luteinizing hormone-induced connexin 43 down-regulation: inhibition of translation. Endocrinology. 2004;145(4):1617–24.
29. Granot I, et al. Connexin43 in rat oocytes: developmental modulation of its phosphorylation. Biol Reprod. 2002;66(3):568–73.
30. Vozzi C, et al. Involvement of connexin 43 in meiotic maturation of bovine oocytes. Reproduction. 2001;122(4):619–28.
31. Berisha B, et al. Expression and Localization of Gap Junctional Connexins 26 and 43 in Bovine Periovulatory Follicles and in Corpus Luteum during different functional stages of Oestrous cycle and pregnancy. Reprod Domest Anim. 2009;44(2):295–302.
32. Qi X, et al. Gut microbiota-bile acid-interleukin-22 axis orchestrates polycystic ovary syndrome. Nat Med. 2019;25(8):1225–33.

Publisher's Note